

# Radiation From a Uniformly Moving Charge in an Anisotropic, Two Component Plasma

S. R. Seshadri<sup>1</sup> and H. S. Tuan

Gorden McKay Laboratory, Harvard University, Cambridge, Mass.

(Received September 24, 1964; revised November 10, 1964)

The effect of motion of heavy ions on the radiation characteristics of a point charge moving with uniform velocity along the direction of the external magnetic field in a plasma is investigated. For the case of stationary ions, two modes are found to be excited up to zero frequencies for values of the normalized strength of the external magnetic field above a certain minimum value. The result of inclusion of the motion of heavy ions is that the ordinary mode has a resonance at the so-called lower hybrid resonant frequency below which it is not excited and the extraordinary mode is excited up to zero frequencies even for very small values of the normalized strength of the external magnetic field. The power radiated in the ordinary mode in the neighborhood of the lower as well as the upper hybrid resonant frequencies is relatively large. The frequency and the angular spectrum of the emitted radiation as well as the direction of the Cerenkov rays are evaluated for some typical parameter values which include those usually obtained in the exosphere.

## 1. Introduction

A point charge moving with a uniform velocity in free-space does not radiate in view of the constraint that its velocity cannot exceed the phase velocity  $c_0$  of the electromagnetic waves in the medium. On the other hand, a point charge moving in a material medium with a uniform velocity less than  $c_0$  can radiate provided its velocity is greater than the phase velocity of the electromagnetic waves in that medium. This radiation is the well-known Cerenkov radiation. An excellent treatment of the general field of Cerenkov radiation may be found in the book by Jelley [1958] and the review articles by Bolotovskii [1957, 1961].

A cold plasma in a magnetic field is equivalent to a dielectric, and Cerenkov radiation is possible in such a medium. However, in a cold plasma without external magnetic field, the phase velocity of the electromagnetic waves is always greater than  $c_0$  with the result, Cerenkov radiation is not emitted in an isotropic plasma. But in an anisotropic plasma, Cerenkov radiation is possible. Kolomenskii [1956] and Sitenko and Kolomenskii [1956] have examined some aspects of the problem of radiation by a charged particle moving with a uniform velocity along the direction of the external magnetic field in a plasma. In their papers, Kolomenskii and Sitenko have not systematically investigated the frequency spectrum of the ordinary and the extraordinary modes nor have they given any consideration to the angular distribution of the radiated energy. McKenzie [1963] has given a thorough treatment of the Cerenkov radiation in a magneto-ionic medium with emphasis on its application to the gen-

eration of low-frequency electromagnetic radiation in the exosphere by the passage of charged corpuscular streams. The present authors [Tuan and Seshadri, 1963] have also given a treatment of the problem of radiation from a point charge moving with a uniform velocity along the direction of the external magnetic field in a plasma. It was found [Tuan and Seshadri, 1963] that for certain parameters both the ordinary and the extraordinary modes were emitted up to zero frequencies. All the foregoing treatments of the Cerenkov radiation in a magneto-ionic medium are based on an idealization in which the motion of the heavy ions is neglected. It is reasonable to neglect the ion motion for frequencies sufficiently greater than the plasma and the gyro-magnetic frequency of the ions. But for lower frequencies, it is not legitimate to ignore the ion motion. It is therefore of interest to study the effect of the motion of the heavy ions on the low-frequency spectrum of the radiation emitted by a uniformly moving charged particle in an anisotropic plasma.

In this paper, the radiation characteristics of a point charge moving with uniform velocity along the direction of the static magnetic field are investigated for the case of the plasma in which the motion of the heavy ions is taken into account. The method employed in this paper is different from those previously employed [McKenzie, 1963; Tuan and Seshadri, 1963]. In general, the emitted radiation is found to consist of two modes. The dispersion relations of these modes are analyzed in detail with a view to finding out the influence of the heavy ions on the low-frequency spectrum of the two modes. The frequency and the angular spectrum as well as the directions of the Cerenkov rays are examined. Numerical results are evaluated for some typical parameters of interest.

<sup>1</sup> Present address: Applied Research Laboratory, Sylvania Electronic Systems, 40 Sylvan Road, Waltham, Mass.

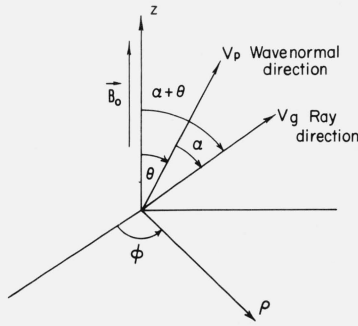


FIGURE 1. Geometry of the problem.

## 2. Statement of the Problem

Consider a fully ionized, homogeneous plasma of infinite extent. For the sake of simplicity, the plasma is idealized to be a lossless and macroscopically neutral mixture of a gas of electrons and a single species of ions in which compressional effects due to finite temperature are neglected. An external magnetic field  $B_0$  is assumed to be uniformly impressed throughout the plasma in the  $z$ -direction, where  $\rho$ ,  $\phi$ , and  $z$  form a cylindrical coordinate system (fig. 1). It is desired to investigate the radiation characteristics of a point charge moving uniformly in the plasma medium along the direction of the external magnetic field. Let

$$q = q_0 \frac{\delta(\rho)}{2\pi\rho} \delta(z - ut) \quad (1)$$

represent a point charge  $q_0$  moving with a uniform velocity  $u$  along the  $z$ -axis from  $z = -\infty$  to  $z = \infty$  such that it passes through the origin at  $t = 0$ . The current density arising from this uniformly moving charge is given by

$$\vec{J}(\vec{r}, t) = \hat{z} q_0 u \frac{\delta(\rho)}{2\pi\rho} \delta(z - ut), \quad (2)$$

where  $\vec{r}$  represents the position vector of a point in the  $\rho$ ,  $\phi$ , and  $z$ -space. It is assumed that the source (2) is sufficiently weak so that the linearized plasma theory is applicable.

Let  $\vec{E}(\vec{r}, t)$  and  $\vec{H}(\vec{r}, t)$  be, respectively, the electric and the magnetic field vectors. It is convenient to introduce the time Fourier transforms defined by

$$f(\vec{r}, \omega) = \int_{-\infty}^{\infty} f(\vec{r}, t) e^{i\omega t} dt \quad (3)$$

$$f(\vec{r}, t) = \frac{1}{2\pi} \int_{-\infty}^{\infty} f(\vec{r}, \omega) e^{-i\omega t} d\omega \quad (4)$$

to the source (2) and all the field quantities. The Fourier transform of the source (2) is obtained as

$$J_z(\vec{r}, \omega) = q_0 \frac{\delta(\rho)}{2\pi\rho} e^{i\omega z/u}. \quad (5)$$

In the frequency domain, the electric and the magnetic field vectors  $\vec{E}(\vec{r}, \omega)$  and  $\vec{H}(\vec{r}, \omega)$  are known to satisfy the following Maxwell's equations

$$\nabla \times \vec{E}(\vec{r}, \omega) = i\omega\mu_0 \vec{H}(\vec{r}, \omega) \quad (6)$$

$$\nabla \times \vec{H}(\vec{r}, \omega) = -i\omega\epsilon_0 \vec{\epsilon} \cdot \vec{E}(\vec{r}, \omega) + \hat{z} J_z(\vec{r}, \omega), \quad (7)$$

where  $\mu_0$  and  $\epsilon_0$  are the vacuum permeability and dielectric constant. In (7),  $\vec{\epsilon}$  is the familiar relative dyadic dielectric constant used in the magneto-ionic theory and its components are given by the following matrix:

$$\vec{\epsilon} = \begin{bmatrix} \epsilon_1 & i\epsilon_2 & 0 \\ -i\epsilon_2 & \epsilon_1 & 0 \\ 0 & 0 & \epsilon_3 \end{bmatrix}, \quad (8)$$

where

$$\epsilon_1 = 1 - \frac{\omega_{pe}^2}{\omega^2 \alpha_e} - \frac{\omega_{pi}^2}{\omega^2 \alpha_i} \quad (9a)$$

$$\epsilon_2 = \frac{\omega_{pe}^2 \omega_{ce}}{\omega^3 \alpha_e} - \frac{\omega_{pi}^2 \omega_{ci}}{\omega^3 \alpha_i} \quad (9b)$$

$$\epsilon_3 = 1 - \frac{\omega_{pe}^2}{\omega^2} - \frac{\omega_{pi}^2}{\omega^2} \quad (9c)$$

$$\alpha_e = 1 - \frac{\omega_{ce}^2}{\omega^2} \quad (9d)$$

$$\alpha_i = 1 - \frac{\omega_{ci}^2}{\omega^2}. \quad (9e)$$

In (9),  $\omega_{pe}$  is the plasma frequency, and  $\omega_{ce}$  is the gyro-magnetic frequency of the electrons. Also  $\omega_{pi}$  and  $\omega_{ci}$  are the corresponding quantities for the ions. It is found to be advantageous, though somewhat unconventional, to employ the following normalized frequencies:

$$\Omega = \frac{\omega}{\omega_{pe}}; \quad R = \frac{\omega_{ce}}{\omega_{pe}}. \quad (10)$$

With the above notation, (9a-c) becomes

$$\epsilon_1 = 1 - \frac{1}{\Omega^2 - R^2} - \frac{m}{\Omega^2 - R^2 m^2} \quad (11a)$$

$$\epsilon_2 = \frac{R}{\Omega(\Omega^2 - R^2)} - \frac{Rm^2}{\Omega(\Omega^2 - R^2 m^2)} \quad (11b)$$

$$\epsilon_3 = \frac{\Omega^2 - 1 - m}{\Omega^2} \quad (11c)$$

where

$$m = \frac{m_e}{m_i} \quad (12)$$

and  $m_e$  and  $m_i$  are the masses of an electron and an ion respectively.

In view of (5) and the geometry of the problem it is obvious that the field components are independent of  $\phi$  and depend on  $z$  only through the phase factor  $e^{i\omega z/u}$ , which may be conveniently separated out as follows:

$$f(\vec{r}, \omega) = f(\rho, \omega) e^{i\omega z/u}. \quad (13)$$

The arguments  $\rho, \omega$  of all the functions will be omitted for convenience.

The projection of a vector in the  $\rho$ - $\phi$  plane will be denoted by the subscript  $t$  and  $\hat{z}$  denotes the unit vector in the  $z$ -direction. The longitudinal and the transverse components of (6) and (7) are given by

$$\frac{i}{\rho} \frac{\partial}{\partial \rho} (\rho E_\phi) + \omega \mu_0 H_z = 0 \quad (14a)$$

$$\frac{1}{\rho} \frac{\partial}{\partial \rho} (\rho H_\phi) + i\omega \epsilon_0 \epsilon_3 E_z = J_z \quad (14b)$$

$$-\hat{z} \times \left( \nabla_t E_z - i \frac{\omega}{u} \bar{E}_t \right) = i\omega \mu_0 \bar{H}_t \quad (15a)$$

$$-\hat{z} \times \left( \nabla_t H_z - i \frac{\omega}{u} \bar{H}_t \right) = -i\omega \epsilon_0 \epsilon_1 \bar{E}_t - \omega \epsilon_0 \epsilon_2 \hat{z} \times \bar{E}_t. \quad (15b)$$

On cross multiplying (15a, b) by  $\hat{z}$ , the expressions for  $\hat{z} \times \bar{H}_t$  and  $\hat{z} \times \bar{E}_t$  can be found and these when substituted back in (15a, b) result in two simultaneous equations in  $\bar{E}_t$  and  $\bar{H}_t$ . The solution of these simultaneous equations yields the following expressions for  $\bar{E}_t$  and  $\bar{H}_t$  in terms of  $H_z$  and  $E_z$ :

$$E_\rho = -\frac{\epsilon_2}{\omega \epsilon_0 \epsilon} \frac{\partial}{\partial \rho} H_z + \frac{i c_0^2 \tilde{\epsilon}_1}{\omega u \epsilon} \frac{\partial}{\partial \rho} E_z \quad (16a)$$

$$E_\phi = -i \frac{\partial}{\partial \rho} [M_{11} H_z + M_{12} i E_z] \quad (16b)$$

$$H_\rho = \frac{i \tilde{\epsilon}_1 c_0^2}{\omega u \epsilon} \frac{\partial}{\partial \rho} H_z + \frac{c_0^2 \epsilon_2}{\omega u^2 \mu_0 \epsilon} \frac{\partial}{\partial \rho} E_z \quad (16c)$$

$$H_\phi = \frac{\partial}{\partial \rho} [M_{21} H_z + M_{22} i E_z] \quad (16d)$$

where

$$\tilde{\epsilon}_1 = \epsilon_1 - \frac{c_0^2}{u^2}, \quad \epsilon = \tilde{\epsilon}_1^2 - \epsilon_2^2 \quad (17a)$$

$$M_{11} = \frac{\tilde{\epsilon}_1}{\omega \epsilon_0 \epsilon}, \quad M_{12} = M_{21} = \frac{-\epsilon_2 c_0^2}{\omega u \epsilon}$$

$$M_{22} = \frac{1}{\omega \mu_0} \left[ 1 + \frac{c_0^2 \tilde{\epsilon}_1}{u^2 \epsilon} \right] \quad (17b)$$

and  $c_0 = 1/\sqrt{\mu_0 \epsilon_0}$  is the free-space velocity of electromagnetic waves.

The substitution of (16b and d) respectively in (14a and b) yields a pair of coupled wave equations, which are conveniently written in the matrix notation as follows:

$$[M] \nabla_t^2 [F] + [N] [F] = [S] \quad (18)$$

where

$$\nabla_t^2 = \frac{\partial^2}{\partial \rho^2} + \frac{1}{\rho} \frac{\partial}{\partial \rho} \quad (19a)$$

$$[M] = \begin{bmatrix} M_{11} & M_{12} \\ M_{21} & M_{22} \end{bmatrix}, \quad [F] = \begin{bmatrix} H_z \\ i E_z \end{bmatrix} \quad (19b)$$

$$[N] = \begin{bmatrix} N_1 & 0 \\ 0 & N_2 \end{bmatrix}, \quad [S] = \begin{bmatrix} 0 \\ J_z \end{bmatrix} \quad (19c)$$

$$\text{and } N_1 = \omega \mu_0, \quad N_2 = \omega \epsilon_0 \epsilon_3. \quad (19d)$$

The solution of (18) and the subsequent evaluation of all the physical quantities of interest are carried out by employing the methods first used by one of the authors [Seshadri, 1965b] in the treatment of the Cerenkov radiation in a warm anisotropic plasma.

### 3. Solution of the Coupled Wave Equations (18)

The coupled wave equations (18) may be decoupled into two separate wave equations by a transformation to a new base. Let

$$[F] = [T] [\Psi] = \begin{bmatrix} T_{11} & T_{12} \\ T_{21} & T_{22} \end{bmatrix} \begin{bmatrix} \Psi_1 \\ \Psi_2 \end{bmatrix}. \quad (20)$$

The substitution of (20) into (18) and the premultiplication by  $[T]^{-1}[M]^{-1}$  yields

$$\nabla^2 [\Psi] + [T]^{-1}[M]^{-1}[N][T] [\Psi] = [T]^{-1}[M]^{-1}[S]. \quad (21)$$

The matrix  $[M]^{-1}[N]$  may be shown to possess two distinct eigenvalues  $k_1^2$  and  $k_2^2$ , and hence,  $[T]$  may be chosen in such a way as to diagonalize  $[M]^{-1}[N]$  with the following result:

$$[\nabla^2 + k_n^2] \Psi_n = -S_n \frac{\delta(\rho)}{2\pi\rho} \quad \text{for } n=1, 2. \quad (22)$$

With the help of (5), (13), and the right side of (21), it is found that

$$\begin{bmatrix} S_1 \\ S_2 \end{bmatrix} = -q_0 [T]^{-1} [M]^{-1} \begin{bmatrix} 0 \\ 1 \end{bmatrix}. \quad (23)$$

The solution of (22) is easily seen to given by

$$\psi_n(\rho) = \frac{i}{4} S_n H_0^{(m)}(k_n \rho); \quad n=1, 2 \text{ and } m=1 \text{ or } 2. \quad (24)$$

The outward power radiated per unit area is given by

$$\bar{S}(\bar{r}, t) = \bar{E}(\bar{r}, t) \times \bar{H}(\bar{r}, t). \quad (25a)$$

Therefore, the total power radiated in the radial direction per unit area and per unit frequency interval is easily obtained with the help of (3), (4), (13), and (25a) to be given by

$$\begin{aligned} S_\rho(\omega) &= \frac{\hat{\rho}}{2\pi} \operatorname{Re} \bar{E}(\bar{\rho}, \omega) \times \bar{H}^*(\rho, \omega) \\ &= \frac{1}{2\pi} \operatorname{Re} [E_\phi(\rho, \omega) - iH_\phi(\rho, \omega)] \begin{bmatrix} H_z(\rho, \omega) \\ iE_z(\rho, \omega) \end{bmatrix}. \end{aligned} \quad (25b)$$

From (16b, d), it follows that

$$\begin{bmatrix} E_\phi(\rho, \omega) \\ -iH_\phi(\rho, \omega) \end{bmatrix} = -i \begin{bmatrix} M_{11} & M_{12} \\ M_{21} & M_{22} \end{bmatrix} \frac{\partial}{\partial \rho} \begin{bmatrix} H_z(\rho, \omega) \\ iE_z(\rho, \omega) \end{bmatrix}. \quad (26)$$

The substitution of (26) in (25b) and the use of (20) yields

$$S_\rho(\omega) = \frac{1}{2\pi} \operatorname{Im} \begin{bmatrix} \frac{\partial \Psi_1}{\partial \rho} & \frac{\partial \Psi_2}{\partial \rho} \end{bmatrix} [T]^\dagger [M] [T]^* \begin{bmatrix} \Psi_1^* \\ \Psi_2^* \end{bmatrix}. \quad (27a)$$

Since the matrix  $[M]^{-1}[N]$  is real, it follows that its eigenvalues  $k_1^2$  and  $k_2^2$  are either purely real or complex conjugates of each other. When the eigenvalues are complex, the corresponding wave functions are seen from (24) to either increase or decrease exponentially. The exponentially growing solution is ruled out from physical considerations and the exponentially decaying solution will not give rise to any radiation. The interest is therefore in the ranges of the parameter values for which the eigenvalues are real. For the case of real eigenvalues,  $[T]$  is real and hence (27a) becomes

$$S_\rho(\omega) = \frac{1}{2\pi} \operatorname{Im} \begin{bmatrix} \frac{\partial \Psi_1}{\partial \rho} & \frac{\partial \Psi_2}{\partial \rho} \end{bmatrix} [T]^\dagger [M] [T] \begin{bmatrix} \Psi_1^* \\ \Psi_2^* \end{bmatrix}. \quad (27b)$$

It was shown that

$$[T]^{-1} [M]^{-1} [N] [T] = \begin{bmatrix} k_1^2 & 0 \\ 0 & k_2^2 \end{bmatrix}. \quad (27c)$$

On premultiplying both sides of (27c) by

$$[A] = [T]^\dagger [M] [T] = \begin{bmatrix} a_{11} & a_{12} \\ a_{21} & a_{22} \end{bmatrix} \quad (28)$$

it is found that

$$\begin{aligned} [B] &= \begin{bmatrix} b_{11} & b_{12} \\ b_{21} & b_{22} \end{bmatrix} = [T]^\dagger [N] [T] \\ &= \begin{bmatrix} a_{11} & a_{12} \\ a_{21} & a_{22} \end{bmatrix} \begin{bmatrix} k_1^2 & 0 \\ 0 & k_2^2 \end{bmatrix}. \end{aligned} \quad (29)$$

From (29) it follows that

$$b_{11} = a_{11}k_1^2, \quad b_{22} = a_{22}k_2^2, \quad (30a)$$

$$b_{12} = a_{12}k_2^2, \quad b_{21} = a_{21}k_1^2. \quad (30b)$$

It is known from (17) and (19) that  $[M]$  and  $[N]$  are symmetric, and therefore it follows that  $[A]$  and  $[B]$  are also symmetric. If the eigenvalues  $k_1^2$  and  $k_2^2$  are distinct, since  $b_{12} = b_{21}$  and  $a_{12} = a_{21}$ , it follows from (30b) that  $a_{12} = a_{21} = b_{12} = b_{21} = 0$ . Consequently, it is found from (27b) and (28) that

$$S_\rho(\omega) = \frac{1}{2\pi} \operatorname{Im} \left[ a_{11} \Psi_1^* \frac{\partial \Psi_1}{\partial \rho} + a_{22} \Psi_2^* \frac{\partial \Psi_2}{\partial \rho} \right]. \quad (31)$$

Since the radiation is circularly symmetrical about the direction of motion of the charge, namely the z-axis, the total power radiated per unit path length and per unit frequency interval is obtained from (31) to be given by

$$I(\omega) = 2\pi\rho S_\rho(\omega) = \rho \operatorname{Im} \left[ a_{11} \Psi_1^* \frac{d\Psi_1}{d\rho} + a_{22} \Psi_2^* \frac{d\Psi_2}{d\rho} \right]. \quad (32)$$

The total power radiated is seen from (32) to be the sum of the powers in the two modes separately. This arises due to the absence of cross terms in (32) and therefore the two wave functions defined by  $\psi_1$  and  $\psi_2$  are orthogonal.

On substituting (24) in (32) and making use of the relation

$$\operatorname{Im} H_0^{(m)*}(x) H_0^{(m)'}(x) = (-1)^{m-1} \frac{2}{\pi x} \quad (33)$$

it may be shown that

$$\begin{aligned} I(\omega) &= \sum_{n=1, 2} (-1)^{m-1} a_{nn} \frac{|S_n|^2}{8} \\ &= \sum_n (-1)^{m-1} \frac{b_{nn}}{k_n^2} \frac{|S_n|^2}{8}. \end{aligned} \quad (34)$$

For each mode, which corresponds to different values of  $n$ ,  $m$  is chosen to be either 1 or 2 depending on whether the corresponding value of  $b_{nm}$  is positive or negative. For a propagating mode, the value of  $k_n^2$  is positive and with the above choice of  $m$ ,  $I(\omega)$  given in (34) will be positive. Thus the fulfillment of the radiation condition, which requires a net outward flow of power at large distances from the source, is ensured.

#### 4. Dispersion Relations

Since  $k_1^2$  and  $k_2^2$  are the two eigenvalues of  $[M]^{-1}[N]$ , it is obvious that  $k_1^{-2} = V_1^2/\omega^2$  and  $k_2^{-2} = V_2^2/\omega^2$  are the eigenvalues of  $[N]^{-1}[M]$ , where  $V$  is the velocity of phase propagation in the radial ( $\rho$ ) direction. Using (19b, c),  $V^2$  may be easily shown to satisfy the following quadratic equation:

$$V^4 + AV^2 + B = 0, \quad (35)$$

where

$$A = -\omega^2 \left( \frac{M_{11}}{N_1} + \frac{M_{22}}{N_2} \right) \quad (36a)$$

and

$$B = \frac{\omega^4}{N_1 N_2} (M_{11} M_{22} - M_{12} M_{21}). \quad (36b)$$

The dispersion equation (35) which specifies the phase velocity  $V$  for propagation in the direction perpendicular to that of the motion of the charge can also be derived in a much simpler way, as shown in the appendix.

The use of (17a, b) and (19d) in (36a and b) yields, after some simplification, the following expressions for  $A$  and  $B$ :

$$A = \frac{u^2}{\epsilon_3} \frac{[\epsilon_1 + \epsilon_3 - \beta^2(\epsilon_1 \epsilon_3 + \epsilon_1^2 - \epsilon_2^2)]}{[1 - 2\epsilon_1 \beta^2 + (\epsilon_1^2 - \epsilon_2^2)\beta^4]} \quad (37a)$$

and

$$B = \frac{u^4 \epsilon_1}{\epsilon_3} \left[ 1 - 2\epsilon_1 \beta^2 + (\epsilon_1^2 - \epsilon_2^2)\beta^4 \right]^{-1} \quad (37b)$$

where

$$\beta = \frac{u}{c_0}. \quad (37c)$$

The solutions of (35) are given by

$$V_{1,2}^2 = -\frac{A}{2} \pm \frac{\epsilon_1}{|\epsilon_1|} \sqrt{(A/2)^2 - B} \quad (38)$$

where the subscripts 1 and 2 correspond to the positive and the negative signs in (38) and denote ordinary and extraordinary, respectively. The factor  $\epsilon_1/|\epsilon_1|$  is introduced in front of the radical to ensure the continuity of  $V_2$  across the line  $\epsilon_1 = 0$ . It is obvious that propagating waves are generated only in the ranges of parameters for which  $V^2$  is positive real. From (38)

positive, real values of  $V^2$  are seen to be obtained only in the following two cases:

*Case 1*  $B < 0$ . For this case,  $|\sqrt{(A/2)^2 - B}| > |\frac{A}{2}|$

and hence  $V_1^2$  only is positive real, with the result that only the ordinary mode is excited in this range.

*Case 2*  $B > 0$ ,  $A < 0$  and  $\left(\frac{A}{2}\right)^2 > B$ . It can be easily

shown that for this case  $V_1^2$  and  $V_2^2$  are both positive real and hence both the ordinary and the extraordinary modes are excited.

It is desired to find the ranges of the parameters  $\Omega$  and  $R$  (given by (10)) which correspond to the above two cases. In this way, the values of the parameters  $\Omega$  and  $R$  for which each of the two modes are generated can be determined.

In most cases, the Alfvén wave velocity  $V_\alpha = c_0 R \sqrt{m}$  is very much smaller than the free-space electromagnetic wave velocity  $c_0$ . Also the mass ratio  $m$  is very much smaller than unity. Consequently, in what follows,  $m$  and  $R^2 m$  are legitimately neglected in comparison with unity.

The parametric equations for  $A = \infty$ ,  $B = \infty$ ,  $A = 0$ , and  $B = 0$  may be easily shown to be given by the following curves in the  $\Omega^2 - R^2$  space:

$$L_1: \epsilon_3 = 0 \quad \text{for } A = \infty \text{ and } B = \infty$$

$$L_2: 1 = (\epsilon_1 \pm \epsilon_2)\beta^2 \quad \text{for } A = \infty \text{ and } B = \infty$$

$$L_3: \epsilon_1 = 0 \quad \text{for } B = 0$$

$$L_4: \epsilon_1 + \epsilon_3 - \beta^2(\epsilon_1 \epsilon_3 + \epsilon_1^2 - \epsilon_2^2) = 0 \quad \text{for } A = 0.$$

With the help of (11a, c), the curves  $L_1 - L_4$  are shown to be given by the following parametric equations

$$L_1: \Omega^2 = 1 + m \quad (39a)$$

$$L_2: \left[ \Omega^2 - R^2 m + \frac{(1+m)\beta^2}{1-\beta^2} \right]^2 = \Omega^2 R^2 (1-m)^2 \quad (39b)$$

$$L_3: \Omega^4 - \Omega^2(1 + R^2 + m + R^2 m^2) + R^2 m(1 + m + R^2 m) = 0 \quad (39c)$$

$$L_4: 2\Omega^6(1-\beta^2) - 2\Omega^4\{(1+m)(1-2\beta^2) + R^2(1+m^2)(1-\beta^2)\} + \Omega^2[\{2m^2R^4 + (1+m)(1+m+m^2)R^2\} - \beta^2\{R^2m(1+m+R^2m) + (1+m)^2 + (1+m)(1+m^2)R^2 + (1+m+R^2m)^2\}] - m^2R^4(1+m) + \beta^2R^2m(1+m)(1+m+R^2m) = 0. \quad (39d)$$

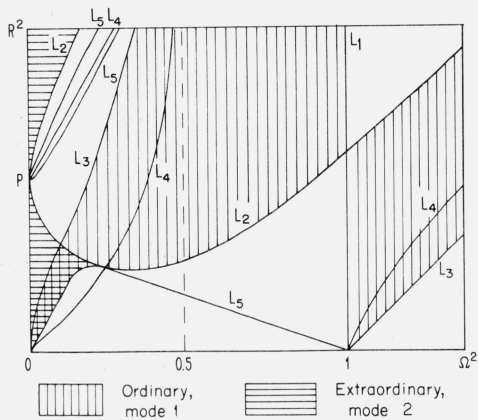


FIGURE 2a. Qualitative sketch of the regions of propagation of the two modes for a two component plasma.

In a similar manner, after some manipulations, it can be established that  $(A/2)^2 - B = 0$  is specified by the following parametric equation:

$$L_5: R^2[(1 - \beta^2)(1 + m^3)\Omega^2 - m^2(1 + m)(1 - \beta^2)R^2 + m(1 + m)^2\beta^2]^2 = 4\beta^2(1 - m^2)^2(1 + m - \Omega^2)\Omega^4. \quad (39e)$$

In figure 2a are sketched the curves  $L_1 - L_5$  which are seen to divide the  $\Omega^2 - R^2$  space into several regions inside which the signs of  $A$ ,  $B$ , and  $(A/2)^2 - B$  do not change. The term  $A$  changes sign only on crossing the curves corresponding to  $A = 0, \infty$ ; i.e.,  $L_1, L_2$ , and  $L_4$ . Similarly,  $B$  changes sign on crossing the curves corresponding to  $B = 0, \infty$ ; i.e.,  $L_1, L_2$ , and  $L_3$ . Also,  $(A/2)^2 - B$  changes sign on crossing the curve  $L_5$ . The signs of  $A$ ,  $B$ , and  $(A/2)^2 - B$  are determined for any one region, and then their signs for the other regions are obtained by inspection. It is then an easy matter to determine the regions of  $\Omega^2 - R^2$  space corresponding to the case 1 ( $B < 0$ , indicated by shading with vertical lines for the ordinary mode and with horizontal lines for the extraordinary mode) and the case 2 ( $B > 0$ ,  $A < 0$ , and  $(A/2)^2 - B > 0$ , indicated by shading with horizontal and vertical lines). In figure 2b, the curves  $L_1 - L_5$  are drawn to scale for the case  $\beta = 10^{-2}$ , and the regions of generation and propagation of the ordinary and the extraordinary modes are indicated by shading with vertical and horizontal lines, respectively.

In order to assess the effect of the motion of the heavy ions on the frequency ranges of excitation of the two modes, it is convenient to study briefly the limiting case of stationary ions, that is  $m = 0$ . For this case, the parametric equations of the curves  $L_1 - L_5$  reduce to the following:

$$L_{10}: \Omega^2 = 1 \quad (40a)$$

$$L_{20}: \left[ \Omega^2 + \frac{\beta^2}{1 - \beta^2} \right]^2 = \Omega^2 R^2 \quad (40b)$$

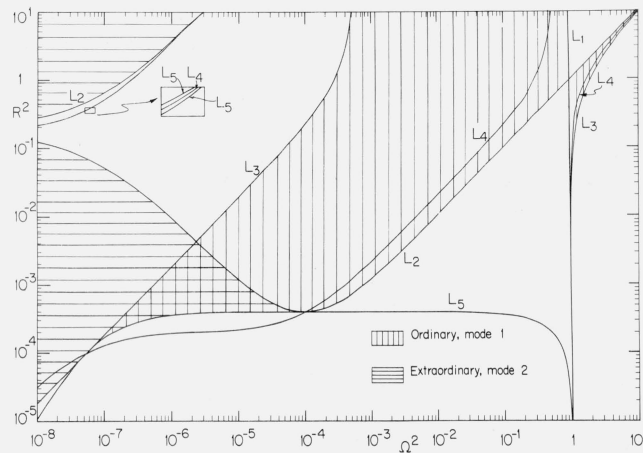


FIGURE 2b. Regions of propagation of the two modes for a two component plasma for  $\beta = u/c_0 = 10^{-2}$ .

$$L_{30}: \Omega^2 = 0; \Omega^2 = 1 + R^2 \quad (40c)$$

$$L_{40}: \Omega^2 = 0;$$

$$R^2 = (\Omega^2 - 1) \left( \Omega^2 + \frac{\beta^2}{1 - \beta^2} \right) / \left( \Omega^2 - \frac{1}{2} \right) \quad (40d)$$

$$L_{50}: R^2 = \frac{4\beta^2}{(1 - \beta^2)^2} (1 - \Omega^2). \quad (40e)$$

In figure 3, the curves  $L_{10} - L_{50}$  are depicted. The regions of generation and propagation of the ordinary and the extraordinary modes are obtained as before and are indicated, as in the case of the two component plasma, by shading with vertical and horizontal lines, respectively.

A comparison of figures 2a and 3 shows that the inclusion of motion of heavy ions considerably modifies the low-frequency end of the spectrum. The curve  $L_3$  is seen to have two branches,  $L'_3$  and  $L''_3$ , whose parametric equations are obtained to be given approximately by  $\Omega^2 = R^2 m / (1 + R^2 + m)$  and  $\Omega^2 = 1 + m + R^2$ , respectively. It may be noted that  $L'_3$  and  $L''_3$  represent the equations for the lower and the upper hybrid resonant frequencies, respectively [Stix, 1962]. It is seen that the motion of the heavy ions alters the radiation characteristics of a uniformly moving point charge in the neighborhood of the lower hybrid resonant frequency and lower. The lower hybrid resonant frequency is considerably larger than the ion gyro-magnetic frequency and is of the order of the geometric mean of the electron and the ion gyro-magnetic frequencies. Since the lower hybrid resonant frequency can be in the ELF or the lower end of the VLF band, it becomes necessary to include the motion of the heavy ions in obtaining the low-frequency part of the Cerenkov radiation in a magneto-ionic medium.

From figure 3, it is found that, in an electron plasma with stationary ions, the ordinary and the extraordinary modes are excited up to zero frequencies if the normalized strength of the external magnetic field is above a

certain minimum value which, however, is dependent on the particle speed. When the motion of the heavy ions is included, the ordinary mode is seen to have a resonance at the lower hybrid resonant frequency below which it is not emitted. The range of excitation and propagation of the extraordinary mode continues to extend up to zero frequencies no matter how small the normalized strength of the external magnetic field.

Note that for the special value of  $R^2 = \frac{(1+m)\beta^2}{m(1-\beta^2)}$

the extraordinary mode is not generated. As  $R^2$  moves away from the critical value, the frequency range of excitation of the extraordinary mode increases. Again for very small  $R^2$ , the pass band of the extraordinary mode decreases as  $R^2$  becomes smaller and finally vanishes for  $R^2 = 0$ .

The normalized phase velocity  $V_1/c_0$  and the normalized wave number  $\Omega c_0/V_1$  for the ordinary mode and the corresponding quantities  $V_2/c_0$  and  $\Omega c_0/V_2$  for the extraordinary mode are evaluated numerically for four different values of  $R$ ; namely, 1.0, 0.5, 0.025, and 0.01, and are depicted in figures 4 to 8. A perusal of the figures 4 to 8 reveals the following interesting characteristics for the propagation of the two modes in the radial direction. The ordinary mode has resonance, that is its phase velocity goes to zero, at the lower hybrid resonant frequency  $\Omega \doteq \sqrt{R^2 m / (1 + R^2 + m)}$  and at the upper hybrid resonant frequency  $\Omega \doteq \sqrt{1 + m + R^2}$ . The phase velocity of the ordinary mode increases as the frequency is increased beyond the lower and decreased from the upper hybrid resonant frequencies, respectively.

An examination of the frequency  $\Omega$  versus wave number  $\Omega c_0/V$  diagram shows that, in certain frequency ranges, the radial propagation is "backward" in character in the sense that the phase and the group velocities are of opposite signs. In order for the total radiated power to be outwardly directed, it was found necessary to choose  $m=1$  in certain frequency ranges and  $m=2$  in the other frequency ranges. It was found from the dispersion diagrams that the frequency ranges in which  $m=1$  or 2 coincided exactly with the frequency ranges in which the phase and the group velocities are of the same or opposite signs, respectively. From (24) and the implied time dependence, it follows that  $m=1$  corresponds to waves whose phase and group velocities are directed outwards from the source whereas  $m=2$  corresponds to a wave for which the group velocity is outwardly directed whereas the phase velocity is inwardly directed.

It is found that the ordinary mode is a "forward" wave for  $\Omega^2 > 1 + m$  and is a "backward" wave for  $\Omega^2 < 1 + m$ . The phase velocity of the ordinary mode decreases with the frequency for  $\Omega^2 > 1 + m$  but increases with the frequency for  $\Omega^2 < 1 + m$ . The extraordinary mode is found to be either "forward" or "backward" or partly "forward" and partly "backward" depending on the value of  $R$ . Its phase velocity is found to either increase ( $R=0.025$ ) or decrease ( $R=0.01$ ) with the frequency. It is interesting to note that in the magnetosphere, say at a distance of 10

earth radii from the center of the earth,  $R$  is approximately equal to  $10^{-2}$  and for that value of  $R$ , the phase velocity of the extraordinary mode decreases with the frequency. This feature can be easily seen to account for the "hydromagnetic whistlers" with a rising tone caused by the passage of the solar particles along the earth's magnetic field, in the magnetosphere. In a similar manner, the ordinary mode for  $\Omega^2 < 1 + m$  with its phase velocity increasing with the frequency can account for the well-known atmospheric whistlers with decreasing tone.

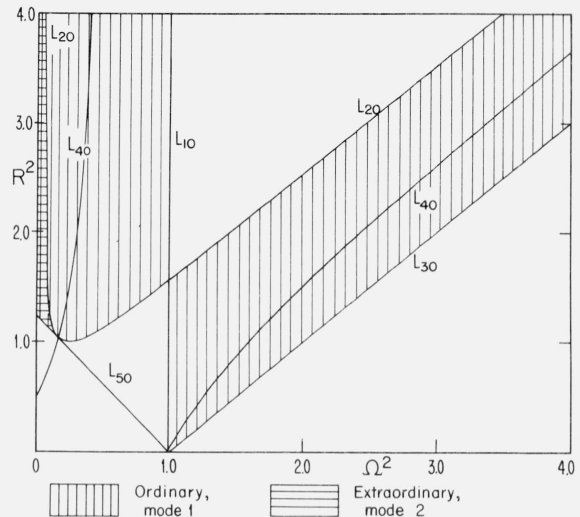


FIGURE 3. Regions of propagation of the two modes for a single component plasma.

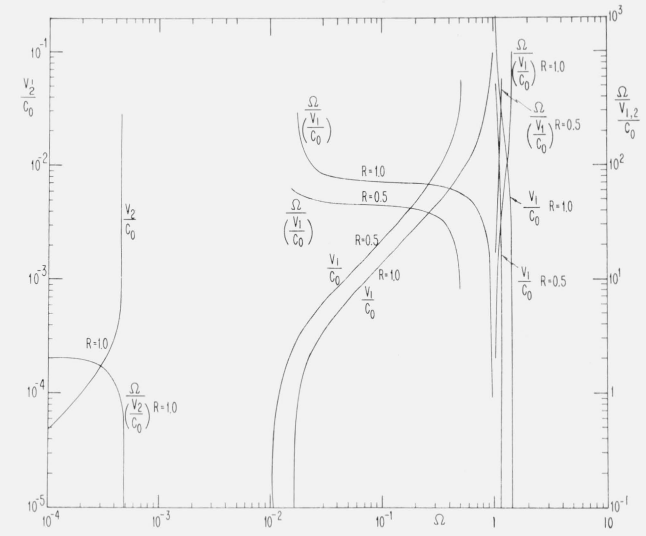


FIGURE 4. Phase velocity and wave number of the ordinary and extraordinary modes for  $R=1.0$  and  $R=0.5$ .

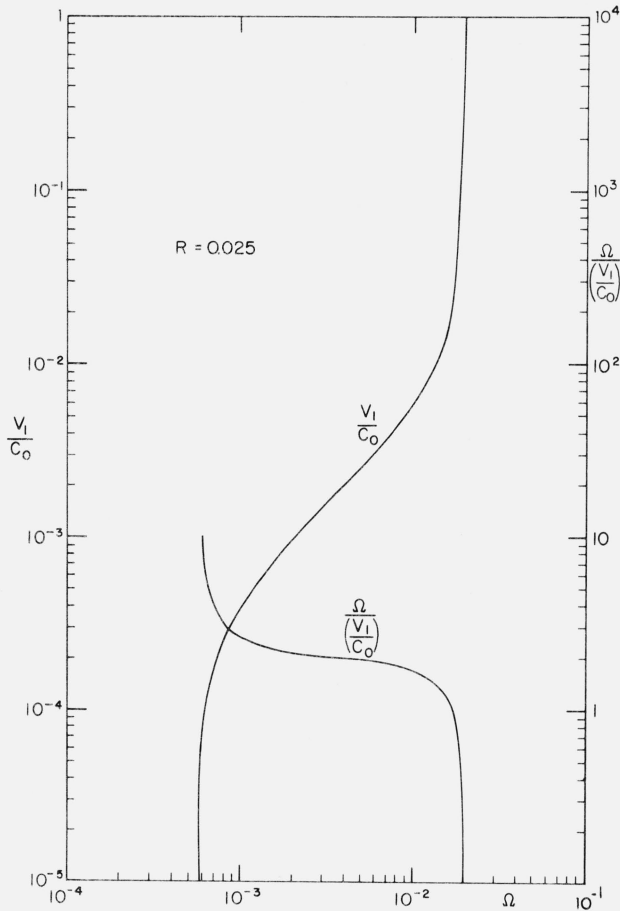


FIGURE 5. Phase velocity and wave number of the ordinary mode for  $R=0.025$  and  $\Omega < 1$ .

## 5. Frequency and Angular Spectrum

The frequency spectrum  $I_1(\omega)$  of the ordinary mode and  $I_2(\omega)$  of the extraordinary mode are defined to be the total power radiated in the respective modes per unit path length and per unit frequency interval. It is of interest to examine the frequency spectrum of the two modes as a function of frequency for some typical values of  $R$ . With the help of (17b), (19d), (20), (23), (29), and (38), it is possible to show from (34), after some standard and straightforward manipulations, that the normalized frequency spectrum  $\tilde{I}_{1,2}(\omega)$  is given by the following expressions:

$$\tilde{I}_1(\Omega) = \frac{I_1(\omega)}{I_0} = \left(\frac{c_0}{V_1}\right)^2 \frac{\beta^2 \Omega^3 G^2}{[R^2 \Omega^4 \epsilon_{1d}^2 + \beta^2 (\Omega^2 - 1) G^2]} \quad (41a)$$

$$\tilde{I}_2(\Omega) = \frac{I_2(\omega)}{I_0} = \left(\frac{c_0}{V_2}\right)^2 \frac{R^2 \Omega^5 \epsilon_{1d}^2}{[R^2 (\Omega^2 - 1) \Omega^2 \epsilon_{1d}^2 + \beta^2 K^2]} \quad (41b)$$

where

$$I_0 = \frac{q_0^2 \omega_0}{8 \epsilon_0 c_0^2} \quad (42a)$$

$$\epsilon_{1N} = \Omega^4 - \Omega^2 (1 + R^2 + m + R^2 m^2) + R^2 m (1 + m + R^2 m) \quad (42b)$$

$$\epsilon_{1d} = (\Omega^2 - R^2) (\Omega^2 - R^2 m^2) \quad (42c)$$

$$G = \frac{1}{\beta^2} \epsilon_{1d}^2 - \epsilon_{1N} \epsilon_{1d} - \left(\frac{V_1}{c_0}\right)^2 \left[ R^2 \Omega^2 - \left(\frac{\epsilon_{1d}}{\beta^2} - \epsilon_{1N}\right)^2 \right] \quad (42d)$$

$$K = \frac{\Omega^2}{\beta^2} \epsilon_{1d} \left(\frac{\epsilon_{1d}}{\beta^2} - \epsilon_{1N}\right) + \left[ R^2 \Omega^2 - \left(\frac{\epsilon_{1d}}{\beta^2} - \epsilon_{1N}\right)^2 \right] \left[ \Omega^2 - (\Omega^2 - 1) \left(\frac{V_2}{c_0}\right)^2 \right] \quad (42e)$$

and  $V_{1,2}/c_0$  is given in (38). The normalized frequency spectrum  $I_1(\omega)$  and  $I_2(\omega)$  are computed from (41a, b) for four different values of  $R$ ; namely,  $R=1.0$ ,  $0.5$ ,  $0.025$ , and  $0.01$ . The normalized speed  $\beta = \frac{u}{c_0}$  is assumed to be equal to  $10^{-2}$ , which is the same as used in the calculations of phase velocity. It is of interest to note that the solar cloud speeds in the exosphere are of the order  $u = 10^{-2} c_0$ . The normalized frequency spectrum of the two modes are plotted in figures 9 to 17. A study of these figures shows that,

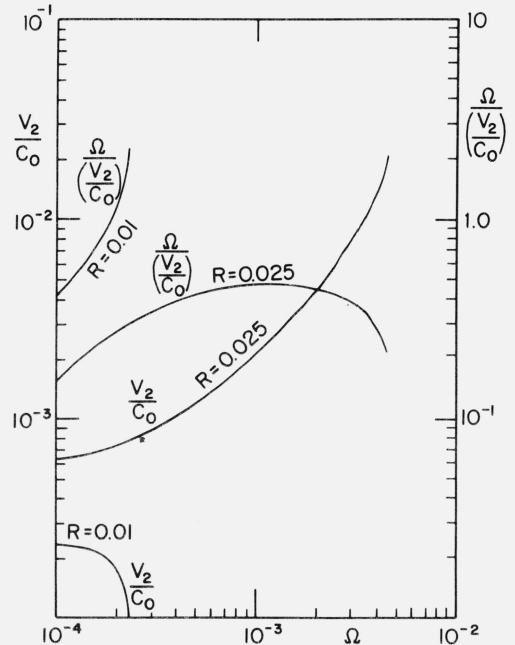


FIGURE 6. Phase velocity and wave number of the extraordinary mode for  $R=0.025$  and  $R=0.01$ .

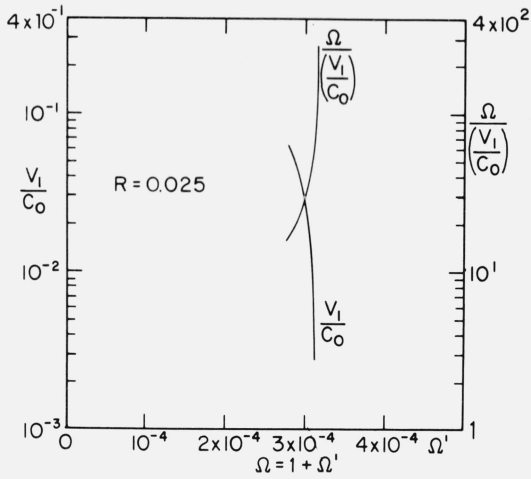


FIGURE 7. Phase velocity and wave number of the ordinary mode for  $R=0.025$  and  $\Omega > 1$ .

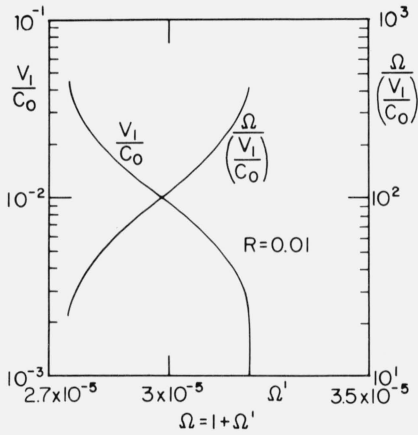


FIGURE 8. Phase velocity and wave number of the ordinary mode for  $R=0.01$ .

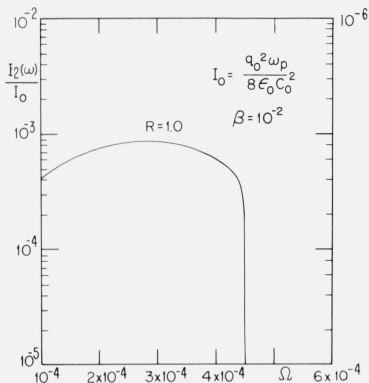


FIGURE 9. Frequency spectrum of the extraordinary mode for  $R=1.0$ .

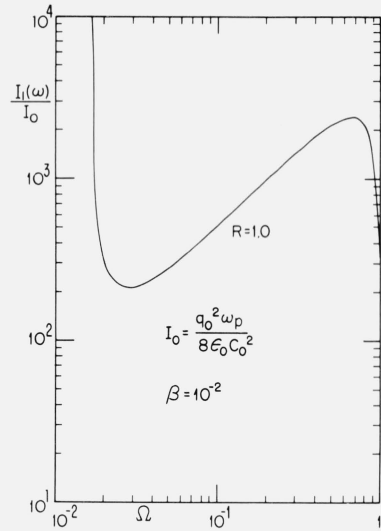


FIGURE 10. Frequency spectrum of the ordinary mode for  $R=1.0$  and  $\Omega < 1$ .

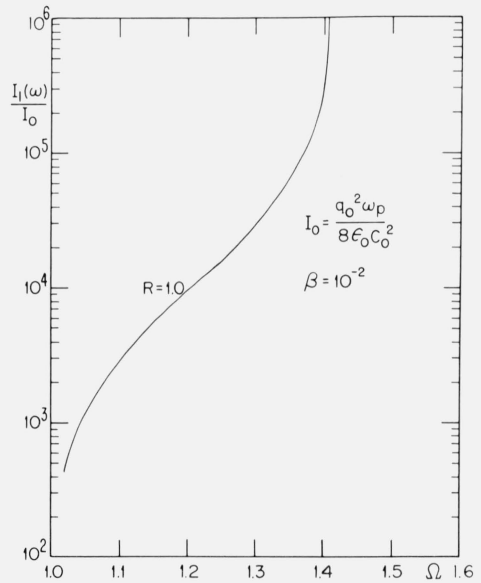


FIGURE 11. Frequency spectrum of the ordinary mode for  $R=1.0$  and  $\Omega > 1$ .

in general, the power radiated is larger for the higher frequencies than for the smaller. It is seen that the frequency spectrum of the ordinary mode becomes infinite at the two hybrid resonant frequencies and on account of this, the total power radiated by a uniformly moving point charge becomes infinite. This difficulty can be overcome in the following manner. At the two hybrid resonant frequencies, the phase velocity in the radial direction goes to zero. The radial direction is transverse to the direction of the external magnetic field. In the neighborhood of the two hybrid

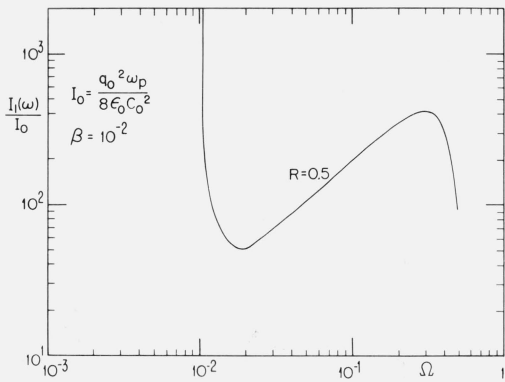


FIGURE 12. Frequency spectrum of the ordinary mode for  $R=0.5$  and  $\Omega < 1$ .

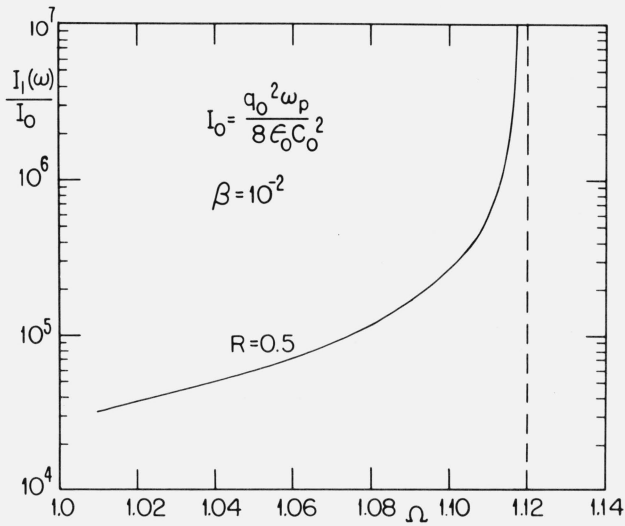


FIGURE 13. Frequency spectrum of the ordinary mode for  $R=0.5$  and  $\Omega > 1$ .

resonant frequencies, since the phase velocity vanishes, the magneto-ionic theory obviously fails. When the phase velocity becomes of the order of the thermal velocity of the charged particles, it is not legitimate to ignore the thermal motion of the particles. A treatment of the wave propagation transverse to the external magnetic field in a two component plasma has been given [Seshadri, 1965a] wherein the effect of the finite temperature of the electrons and the ions has been included. When finite temperature effects are included, it is found that the phase velocity instead of going to zero at the upper and the lower hybrid resonant frequencies, actually levels off to the value of the acoustic velocity in the electron and the ion gas respectively. As a result of this, the frequency spectrum at upper hybrid resonant frequency, instead of becoming infinite, attains only a maximum value which depends on some inverse power of the acoustic velocity  $u_e$  in the electron gas. Similarly, the frequency

spectrum at the lower hybrid resonant frequency attains only a maximum value which depends on some inverse power of the acoustic velocity  $u_i$  in the ion gas. Since  $u_i < u_e$ , the frequency spectrum near the lower hybrid resonant frequency is likely to be higher.

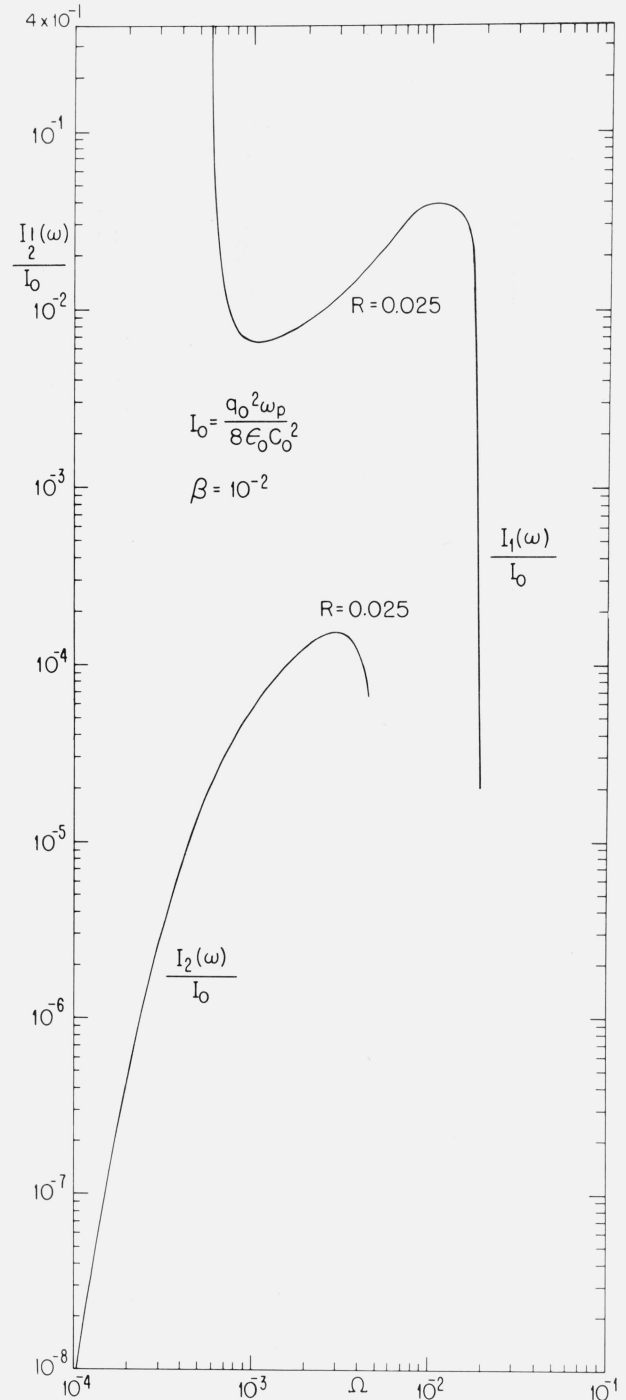


FIGURE 14. Frequency spectrum of the ordinary and the extraordinary modes for  $R=0.025$  and  $\Omega < 1$ .

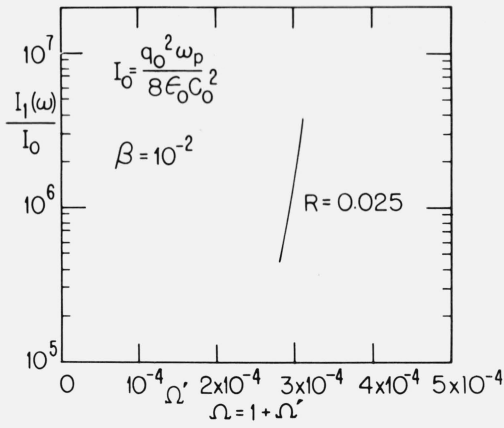


FIGURE 15. Frequency spectrum of the ordinary mode for  $R=0.025$  and  $\Omega > 1$ .

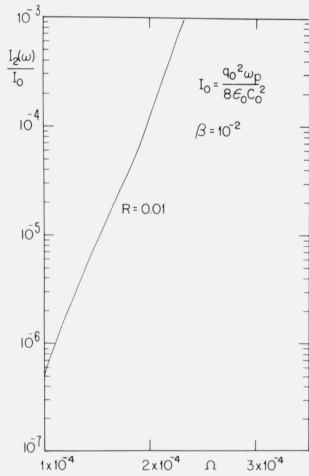


FIGURE 16. Frequency spectrum of the extraordinary mode for  $R=0.01$ .

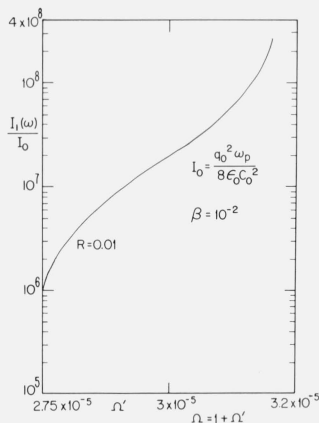


FIGURE 17. Frequency spectrum of the ordinary mode for  $R=0.01$ .

A systematic investigation of the Cerenkov radiation in a warm, anisotropic plasma has been carried out elsewhere by one of the authors [Seshadri, 1965b] for a single component plasma, and in that investigation a finite value has been obtained for the frequency spectrum near the upper hybrid resonant frequency, as anticipated above.

The value of  $R$  over a large part of the earth's exosphere is of the order  $10^{-2}$  and for example, at 4 earth radii from the earth's center,  $R=2 \times 10^{-2}$ , approximately [Mckenzie, 1963]. It is seen from figure 2b that, for  $R$  between  $2 \times 10^{-2}$  to  $6 \times 10^{-2}$ , both the modes are emitted above the lower hybrid resonant frequency over a band which is largest for  $R=2 \times 10^{-2}$  and which continually diminishes as  $R$  is increased to the value  $R=6 \times 10^{-2}$ . It is seen that the power radiated in the ordinary mode is considerably larger than that in the extraordinary mode as can be seen from figure 14. In view of the presence of the lower hybrid resonant frequency, the power radiated in the neighborhood of that frequency is quite high, a fact which is not uncovered in the treatments wherein the ion motion is neglected.

It is of interest to examine the polar diagram of the Cerenkov radiation. The normalized angular spectrum  $I_1(\theta)$  and  $I_2(\theta)$  for the ordinary and the extraordinary modes are evidently given by the relation

$$I_n(\theta) = \tilde{I}_n(\Omega) / \left( 2\pi \sin \theta_n \left| \frac{d\theta}{d\Omega} \right|_n \right) \quad n=1, 2. \quad (43)$$

The angle  $\theta$  between the direction of motion of the charge and the direction of the phase front is easily seen to be given by

$$\tan \theta_n = \beta / (V_n / c_0) \quad n=1, 2. \quad (44)$$

By making use of (38), (41), (43), and (44), the expressions for the normalized angular spectrum  $I_1(\theta)$  and  $I_2(\theta)$  of the modes can be obtained. The details of

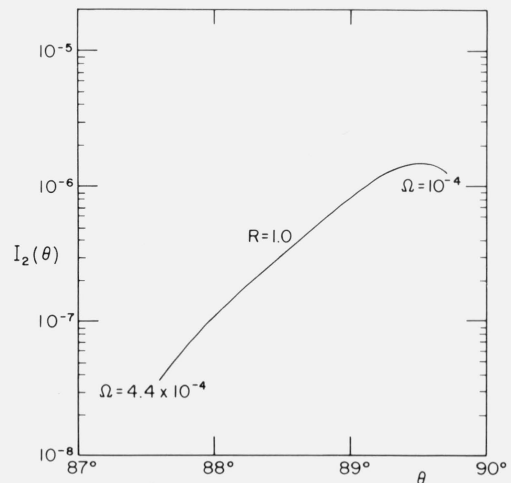


FIGURE 18. Angular spectrum of the extraordinary mode for  $R=1.0$ .

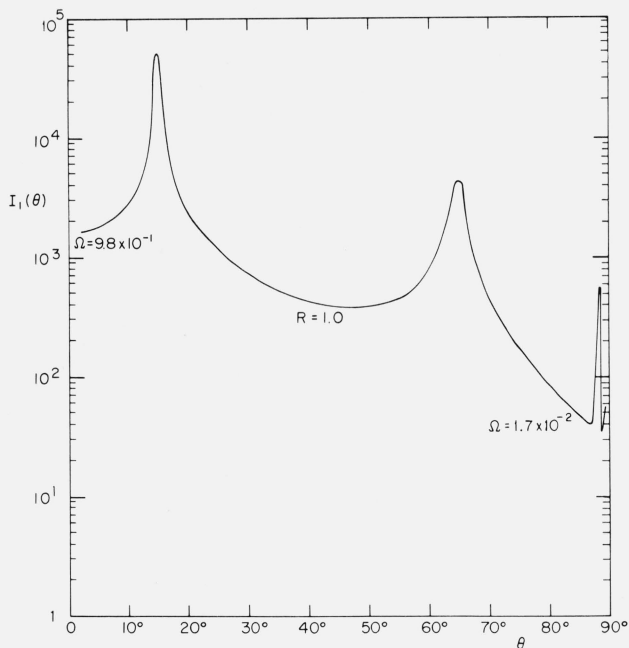


FIGURE 19. Angular spectrum of the ordinary mode for  $R=1.0$  and  $\Omega < 1$ .

these calculations as well as the final expressions, which are quite complicated, are omitted here for the sake of brevity. The numerical results of the angular spectrum of the two modes are given in figures 18 to 24 for the same four values of  $R$  as before and for  $\beta=10^{-2}$ . The polar plot of the Cerenkov radiation shows interesting maxima and minima as a function of the angle made by the direction of the wave front with the direction of motion of charge. It is seen that the two hybrid resonant frequencies correspond to  $\theta=90^\circ$ , as expected. Note from the figures 18 to 24 that the angular spectrum has not been evaluated in certain cases up to very close to the hybrid resonant frequencies.

## 6. Cerenkov Ray Direction

In an anisotropic medium, the direction of the power flow or the Cerenkov ray is different from the direction of the wave normal. It can be shown [Stix, 1962] that the angle  $\alpha$  between the directions of the Cerenkov ray and the wave normal is given by

$$\tan \alpha_n = -\frac{V_n}{c_0} \frac{d}{d\theta} \left( \frac{c_0}{V_n} \right) \quad n = 1, 2 \quad (45)$$

with the result the Cerenkov ray makes an angle  $\theta + \alpha$  with the direction of motion of charge. With the help of (38), (44), and (45), the Cerenkov ray direction specified by  $\theta + \alpha$  corresponding to every wave normal direction  $\theta$  can be computed. The numerical results are obtained for the same four different values of  $R$  as before and for the entire range of frequencies for which emission is possible. The numerical values as

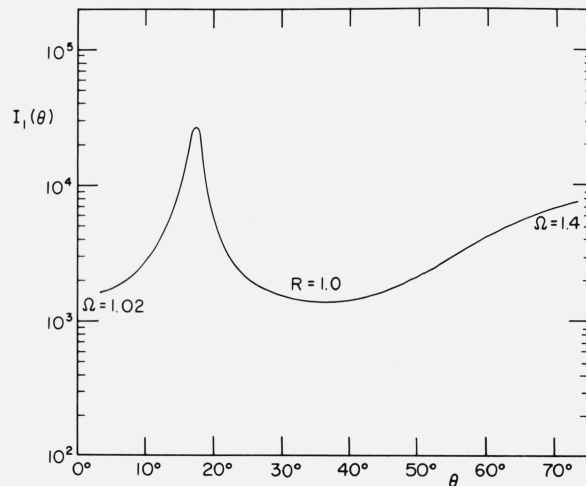


FIGURE 20. Angular spectrum of the ordinary mode for  $R=1.0$  and  $\Omega > 1$ .

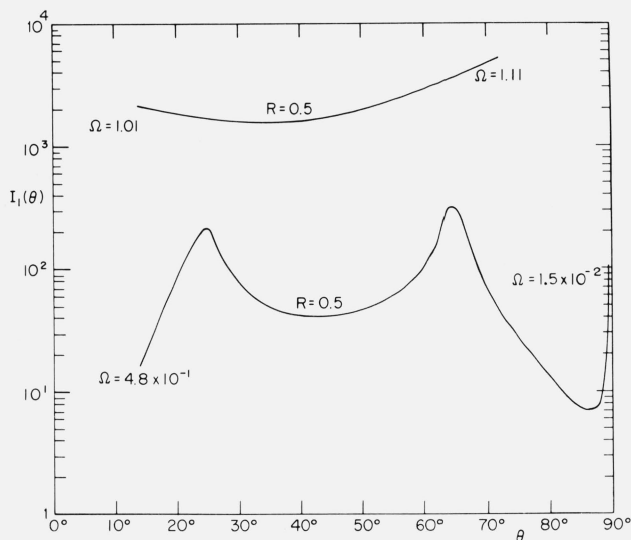


FIGURE 21. Angular spectrum of the ordinary mode for  $R=0.5$ .

depicted in figures 25 to 34 reveal two important features of the Cerenkov ray directions in an anisotropic plasma. In an isotropic medium, the Cerenkov ray directions make only acute angles with the direction of motion of the source whereas in an anisotropic medium such as the one considered in this paper, for appropriate parameter values, the Cerenkov ray makes obtuse angles with the direction of motion of the source, as may be seen from figures 26, 28 to 31, 33, and 34. The second important feature of the Cerenkov ray directions in an anisotropic plasma is that for extremely low frequencies, the ray directions are confined to angles very close to the direction of the external magnetic field, either in the same or in the opposite direction to the motion of the source. It is seen from figure 25 (extraordinary mode,  $10^{-4} < \Omega$

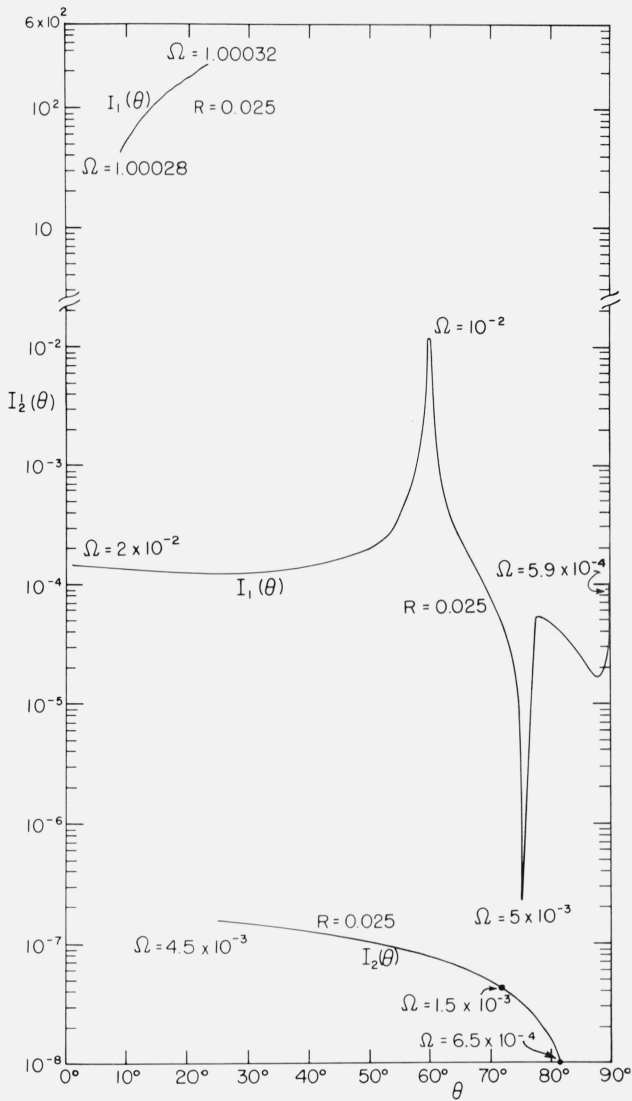


FIGURE 22. Angular spectrum of the ordinary and the extraordinary modes for  $R=0.025$ .

$< 4.4 \times 10^{-4}$ ,  $R=1.0$ ), figure 30 (extraordinary mode,  $10^{-4} < \Omega < 10^{-3}$ ,  $R=0.025$ ), figure 31 (ordinary mode,  $6 \times 10^{-4} < \Omega < 1.5 \times 10^{-3}$ ,  $R=0.025$ ) and figure 33 (extraordinary mode,  $10^{-4} < \Omega < 2.3 \times 10^{-4}$ ,  $R=0.01$ ) that, for the frequency ranges and the appropriate mode type indicated within the brackets, the ray directions are confined to very small angles with the direction of the magnetic field. For larger values of  $R$ , the lower frequency Cerenkov rays are in the same direction as that of the motion of the source as seen from figures 25, 30, and 31. The atmospheric whistlers arising from the solar cloud streaming through the plasma of the exosphere in the direction of the earth's magnetic field are attributed to the ordinary mode (fig. 31) and have their ray directions in the direction of motion of the source. For smaller values of  $R$ , such as for example  $R=0.01$ , which are usually

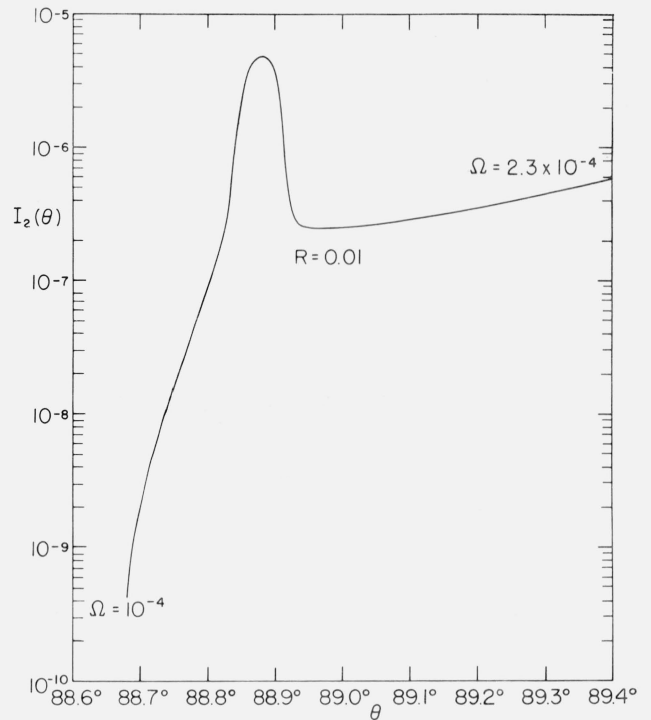


FIGURE 23. Angular spectrum of the extraordinary mode for  $R=0.01$ .

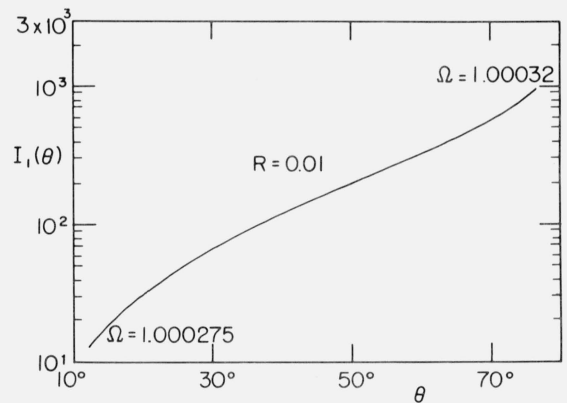


FIGURE 24. Angular spectrum of the ordinary mode for  $R=0.01$ .

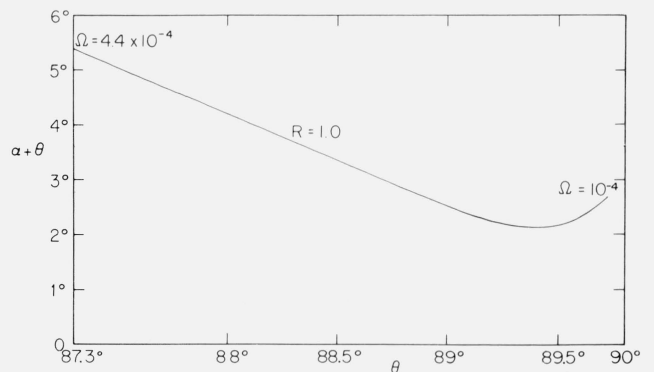


FIGURE 25. Ray direction of the extraordinary mode for  $R=1.0$ .

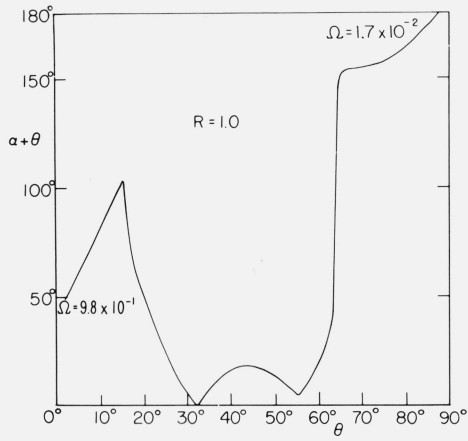


FIGURE 26. Ray direction of the ordinary mode for  $R=1.0$  and  $\Omega < 1$ .

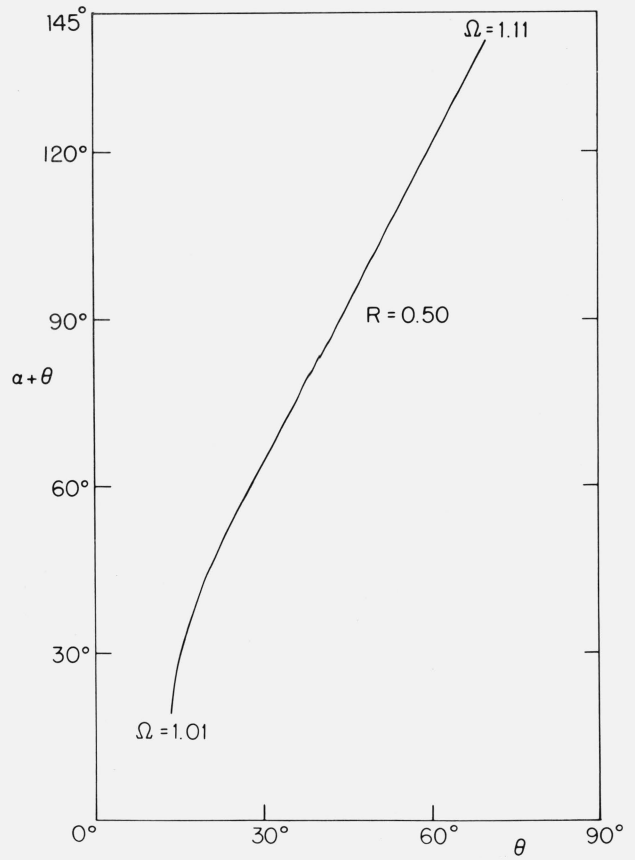


FIGURE 29. Ray direction of the ordinary mode for  $R=0.5$  and  $\Omega > 1$ .

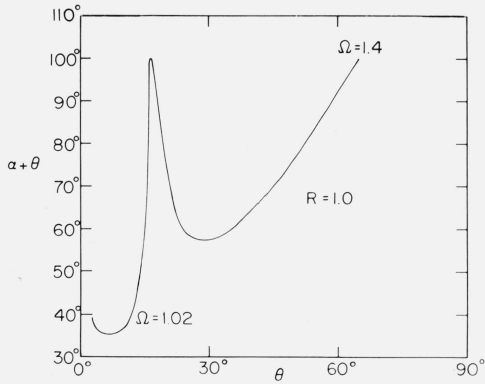


FIGURE 27. Ray direction of the ordinary mode for  $R=1.0$  and  $\Omega > 1$ .

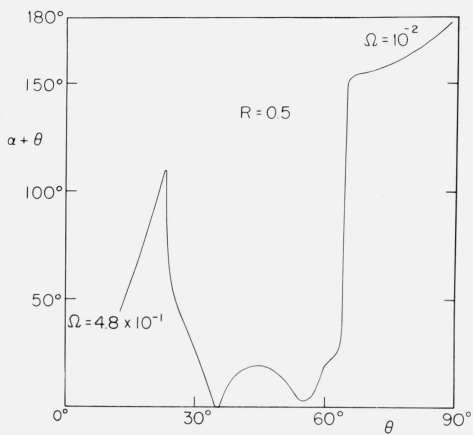


FIGURE 28. Ray direction of the ordinary mode for  $R=0.5$  and  $\Omega < 1$ .

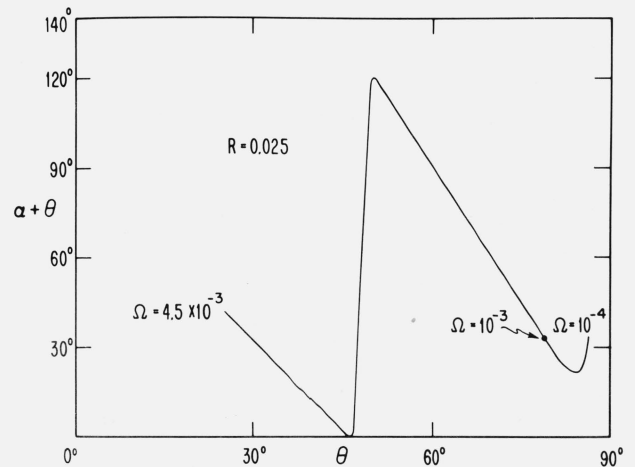


FIGURE 30. Ray direction of the extraordinary mode for  $R=0.025$ .

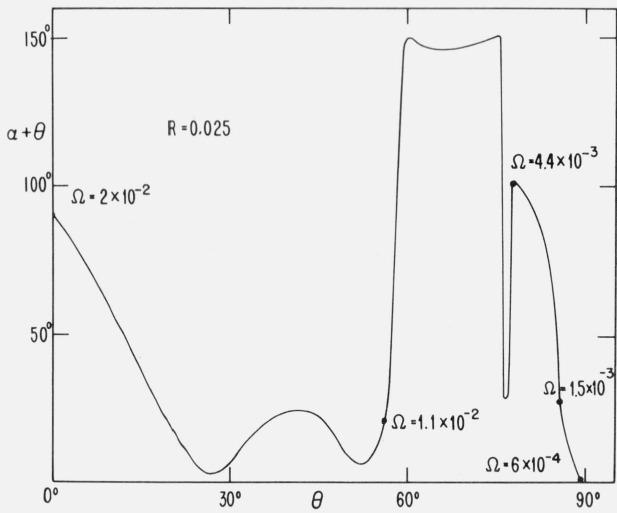


FIGURE 31. Ray direction of the ordinary mode for  $R=0.025$  and  $\Omega < 1$ .

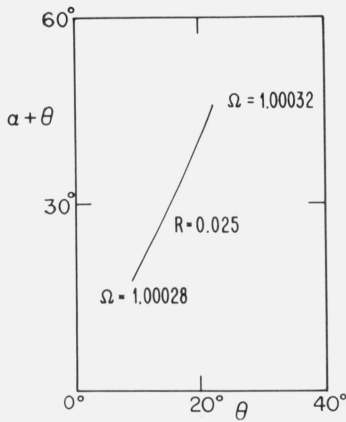


FIGURE 32. Ray direction of the ordinary mode for  $R=0.025$  and  $\Omega > 1$ .

obtained at distances greater than about five earth's radii from the center of the earth, the extremely low-frequency Cerenkov rays are confined to small angles about the direction of the magnetic field but lie in a direction opposite to that of the motion of the source. The sub ELF or the hydromagnetic emissions [Tepley, 1961] are attributed to the extraordinary mode (fig. 33) and have their directions behind the motion of the source. It is seen from figures 25 to 34 that, in certain cases, the ray directions change very rapidly with the wave normal direction and the physical explanation for this behavior is not clear.

To facilitate easy reference, an index to all the figures is provided in table 1 wherein for each value of  $R$ , the frequency ranges of excitation, the mode number, the wave type and the numbers of figures showing the dispersion, the frequency, and the angular spectrum and the ray directions are included.

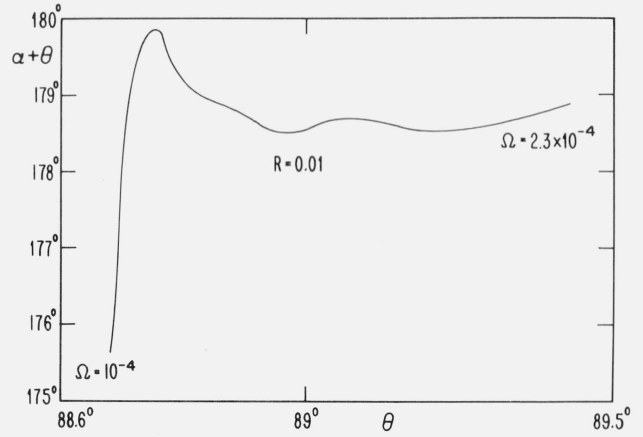


FIGURE 33. Ray direction of the extraordinary mode for  $R=0.01$ .

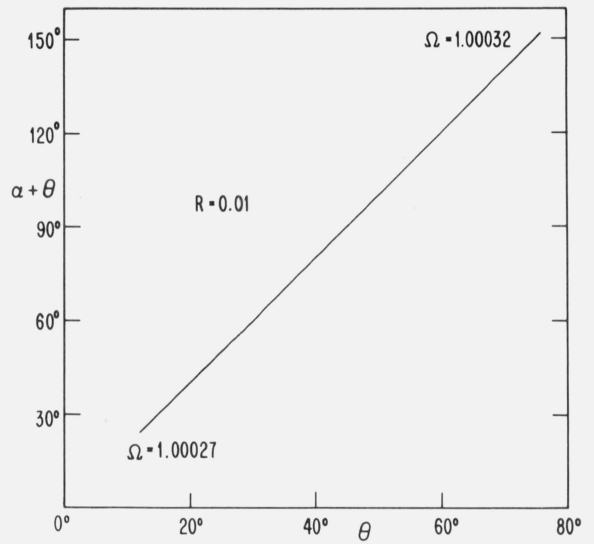


FIGURE 34. Ray direction of the ordinary mode for  $R=0.01$ .

TABLE 1. Index to figures

$R$	Frequency range of excitation	Mode No.	Wave type	Figure number			
				$\frac{V}{c_0} \& \frac{\Omega}{V/c_0}$	Freq. Spect.	Ang. Spect.	$\alpha - \theta$
1.0	$10^{-4}$ to $4.5 \times 10^{-4}$ $\sqrt{2} \times 10^{-2}$ to 1 1 to $\sqrt{2}$	2	Backward	Fig. 4	9	18	25
		1	Backward				
		1	Forward				
0.5	$10^{-2}$ to 0.5 1 to 1.14	1	Backward	4	12	21	28
		1	Forward	4	13	21	29
0.025	$10^{-4}$ to $4.5 \times 10^{-3}$ $6 \times 10^{-4}$ to $2 \times 10^{-2}$ 1 to $\sqrt{1+6 \times 10^{-4}}$	2	Forward-Backward	6	14	22	30
		1	Backward	5	14	22	31
		1	Forward	7	15	22	32
0.01	$10^{-4}$ to $2.3 \times 10^{-4}$ 1 to $\sqrt{1+10^{-4}}$	2	Forward	6	16	23	33
		1	Forward	8	17	24	34

## 7. Concluding Remarks

The characteristics of some of the electromagnetic emissions which are detected both on the earth and by satellite borne receivers suggest Cerenkov type radiation generated by charged particles moving at high speed along the magnetic field lines in the magnetosphere as a possible mechanism. With the purpose of understanding these emissions, considerable investigations of the Cerenkov radiation in a uniform magneto-ionic medium have been carried out. In all these treatments, the ion motion has been omitted. Whereas the neglect of ion motion may be legitimate for the higher end of the VLF band, it is only proper to take into account the motion of heavy ions for the evaluation of the electromagnetic emissions in the lower end of the VLF and ELF bands. Recently, there has been interest in the interpretation of the observed emissions at hydromagnetic frequencies in which range the ion motion certainly plays a dominant role and cannot therefore be neglected.

In this paper, the restriction on the motion of the ions is removed and the theory of Cerenkov radiation in a magneto-ionic medium is extended to apply even to ELF and hydromagnetic frequencies by the inclusion of the motion of the heavy ions. Not only has the analysis of the Cerenkov radiation in a two component magnetoplasma been carried out using a different and somewhat simpler method but some of the special features, such as, for example, the existence of the "backward" wave character of the radial propagation, which have been overlooked previously in the literature, are emphasized in this treatment.

In an anisotropic medium, the direction of power flow and the wave normal direction do not coincide. The radiation condition requires that the net power flow be directed outward from the source. In certain frequency ranges, it is possible for the wave normal direction to be inwardly pointed, giving rise to backward waves. It was found necessary while evaluating the frequency spectrum to require the waves to have inwardly traveling phase fronts for certain frequency ranges to obtain outwardly traveling power. The existence of the backward waves was further confirmed by the examination of the dispersion diagrams, which yielded oppositely directed phase and group velocities in the frequency ranges appropriate to the backward wave regions.

Extensive numerical results on the frequency spectrum, the angular spectrum, and the Cerenkov ray directions are presented for parameter values appropriate to the magnetosphere and for a particle speed of the order of the estimated solar cloud speeds. The power radiated by a single point charge in uniform motion is so small that it cannot account for the observed power levels of low frequency emissions. A realistic estimate of the number density of particles whose coherent emission alone can give the proper order of magnitude for the intensity of the low-frequency emissions will require a detailed examination of the propagation mechanism and the inclusion of the effect of the ionosphere boundary, in addition

to the mechanism of excitation which alone is considered in this treatment.

The authors are grateful to R. W. P. King for his help and encouragement of this research. One of the authors (S. R. Seshadri) is indebted to Ronald V. Row of the Applied Research Laboratory, Sylvania Electronic Systems, Waltham, Mass., for the several instructive discussions.

## 8. Appendix

The dispersion relations for a plane wave propagating at an angle  $\theta$  with respect to the direction of the external magnetic field are given by the following Appleton-Hartree formula [Stix, 1962]

$$A_0 \left( \frac{v_{ph}}{c_0} \right)^4 + A_1 \left( \frac{v_{ph}}{c_0} \right)^2 + A_2 = 0 \quad (A.1)$$

where

$$A_0 = \epsilon_3(\epsilon_1^2 - \epsilon_2^2) \quad (A.2)$$

$$A_1 = -[\epsilon + \epsilon_1 \epsilon_3 - (\epsilon - \epsilon_1 \epsilon_3) \cos^2 \theta] \quad (A.3)$$

$$A_2 = \epsilon_1 - (\epsilon_1 - \epsilon_3) \cos^2 \theta \quad (A.4)$$

and  $v_{ph}$  is the phase velocity of the plane wave in the magneto-ionic medium. If the objective is merely to determine the ranges of the parameters  $\Omega$  and  $R$  in which the propagating waves are excited by a point charge moving with uniform velocity  $u$  in the direction of the external magnetic field, then it is possible and also desirable to start with (A.1) and obtain the dispersion relation (35) specifying the phase velocity  $v$  for propagation in the direction perpendicular to the direction of motion of the charge. It is well known that a charge moving with uniform velocity  $u$  through a medium of refractive index  $c_0/v_{ph}$  will emit Cerenkov radiation at an angle  $\theta$  with respect to its direction of motion if the condition for coherent radiation, namely,

$$u \cos \theta = v_{ph} \quad (A.5)$$

is satisfied. Also, it is easily seen that the phase velocity  $v$  normal to the direction of motion of charge is given by

$$v \sin \theta = v_{ph}. \quad (A.6)$$

With the help of (A.5) and (A.6), it may be shown that

$$v_{ph}^2 = v^2 / (1 + v^2/u^2). \quad (A.7)$$

The elimination of  $\cos \theta$  and  $v_{ph}$  from (A.1)–(A.4) with the help of (A.5) and (A.7) yields (35), after some simplification.

## 9. References

- Bolotovskii, B. M. (1957), The Cerenkov effect in infinite media and in crystals, I and II, *Usp. Fiz. Nauk.* **62**, 201-230.
- Bolotovskii, B. M. (1961), Theory of Cerenkov radiation III, *Soviet Phys. Usp.* **4**, 781-811.
- Jelley, J. V. (1958), *Cerenkov radiation and its applications* (Pergamon Press, London, England).
- Kolomenskii, A. A. (1956), Radiation from a plasma electron in uniform motion in a magnetic field, *Soviet Phys. Doklady* **1**, 133-136.
- Mckenzie, J. F. (1963), Cerenkov radiation in a magneto-ionic medium, *Phil. Trans. Roy. Soc. London Ser. A* **255**, 585-606.
- Seshadri, S. R. (1965a), Radiation propagating transverse to the external magnetic field, from an electromagnetic source in an unbounded plasma, *IEEE Trans. Ant. Prop.* **AP-13**, No. 1, 106-115.
- Seshadri, S. R. (1965b), Cerenkov radiation in a warm, anisotropic plasma, Research Report No. 422, Applied Research Laboratory, Sylvania Electronic Systems, Waltham, Mass.
- Sitenko, A. G. and Kolomenskii, A. A. (1956), Motion of a charged particle in an optically active anisotropic medium I. *Soviet Phys. JETP* **3**, 410-416.
- Stix, T. H. (1962), *The theory of plasma waves* (McGraw-Hill Book Co., Inc., New York, N.Y.).
- Tepley, L. R. (1961), Observations of hydromagnetic emissions, *J. Geophys. Res.* **66**, 1651-1658.
- Tuan, H. S. and Seshadri, S. R. (1963), Radiation from a uniformly moving charge in an anisotropic plasma, *IEEE Trans. Microwave Theory Tech.* **MTT-11**, 462-471.

(Paper 69D5-511)